

Metastable and equilibrium structures on Pt₃Sn(001) studied by STM, RHEED, LEED, and AES

M. Hoheisel, J. Kuntze, S. Speller, A. Postnikov, and W. Heiland
FB Physik, Universität Osnabrück, D-49069 Osnabrück, Germany

I. Spolveri and U. Bardi
Dipartimento di Chimica, Università di Firenze, I-50121 Firenze, Italy
 (Received 6 January 1999; revised manuscript received 1 March 1999)

After sputtering and moderate annealing (600 K) the Pt₃Sn(001) surface shows a $c(2\times 2)$ -LEED pattern with streaky facet spots. The scanning tunneling microscopy (STM) images show pyramidal features that mainly consist of (102) facets, in addition to flat parts between and on top of the pyramids. On the flat parts the dominating feature are triple atomic rows, which probably consist of Pt. According to Auger electron spectroscopy the Sn surface concentration is reduced due to preferential sputtering. Annealing at 1000 K restores the Sn surface concentration and leads to an improved $c(2\times 2)$ -LEED pattern with no facet spots. With the STM the disappearance of the pyramids and the formation of large flat terraces with added single atomic rows along the [100] and [010] surface directions is observed. All steps found are double steps, indicating a strict termination with the mixed Pt/Sn layer. Chemical contrast between Pt and Sn atoms is observed.

[S0163-1829(99)09627-7]

I. INTRODUCTION

The PtSn surfaces are studied for their catalytic properties useful for electro-oxidation of methanol in fuel cells and for hydrocarbon conversion.¹⁻⁴ The low-index single-crystal surfaces especially of Pt₃Sn have been studied by low-energy ion scattering (LEIS),⁵⁻⁹ crystallographic low-energy electron diffraction (LEED),^{10,11} spot-profile-analysis (SPA) LEED (Ref. 9) and x-ray photoelectron spectroscopy (XPD).¹¹ Pt₃Sn crystallizes in the $L1_2$ or Cu₃Au-type structure. Nevertheless, the structures found on the Pt₃Sn surfaces are by no means in all details comparable with the observations of other crystal surfaces of the same crystal type, i.e., Cu₃Au,¹²⁻¹⁶ Ni₃Al,¹⁷⁻¹⁹ or Pt₃Ti.^{20,21}

The low-index surfaces of Pt₃Sn have been found to terminate always with the chemically mixed layer. The LEED patterns of the surfaces are regular $p(2\times 2)$, $c(2\times 2)$, and (1×2) for the (111), (001), and (110) surfaces, respectively.^{10,7} The data of the (110) surface have, however, not yet the same quality as the data of the other two surfaces.⁸ The sputtering causes in all three surfaces a lowering of the Sn surface concentration. The annealing restores the surface concentration by segregation. At intermediate stages of the preparation, other structures are observed, e.g., $(\sqrt{3}\times\sqrt{3}) R30^\circ$ on (111) (Refs. 11, 9, and 22) or (1×3) on (110).^{6,8} The Pt₃Sn(001) surface has been reported to be "disordered" after annealing to temperatures below 1000 K apparent from streaky LEED patterns.⁶⁻⁸

In the present paper we report results based on scanning tunneling microscopy (STM) studies supported by Auger electron spectroscopy (AES), reflection high-energy electron diffraction (RHEED), and LEED observation of the Pt₃Sn(001) surface. A new type of pyramidal structure is found at intermediate annealing temperatures. Atomic row structures are observed up to 1000 K.

II. EXPERIMENT

The preparation of the Pt₃Sn(001)-oriented single crystal has been described in detail elsewhere.¹⁰ The Pt₃Sn alloys are chemically ordered according to x-ray diffraction (XRD) with a lattice parameter of 4.00 Å.¹⁰ The surface is prepared in our Omicron STM 1 system in the preparation chamber by sputtering with clean Ar ions at 500 eV. For the subsequent annealing, the crystal is transferred to the analysis chamber of the instrument. In the analysis chamber AES, RHEED, and LEED can be used in addition to STM. For the AES, we use an electrostatic 180° energy analyzer (Physical Electronics) and the RHEED electron source (Staib). The LEED system is a reversed 4-Grid Omicron type. The screen is also used for the RHEED observations. The patterns are recorded with a video system.

III. RESULTS

After ion bombardment, the surface Sn concentration in the surface region is decreased, as can be seen in Fig. 1, which shows a series of AE spectra with increasing annealing temperature after sputtering. At each temperature level, the crystal was held for 30 min. The spectra were taken after cooling to room temperature. The increase of the Sn concentration with increasing annealing is obvious. Atomic concentrations of Pt and Sn have been calculated via the differentiated $dN(E)/dE$ signals of Pt (241 eV) and Sn (432 eV) using sensitivity factors listed in Ref. 23. Within the limitations of quantification of AES, the final Sn concentration agrees with previous data, i.e., the concentration reaches 25 at. %. The LEED pattern shows at lower annealing temperatures a $c(2\times 2)$ structure with streaks between the main spots as in Fig. 2 [the nomenclature in our case is such that we refer to the unit cell of the substitutionally disordered surface as (1×1)]. The streaks are indeed facet spots that

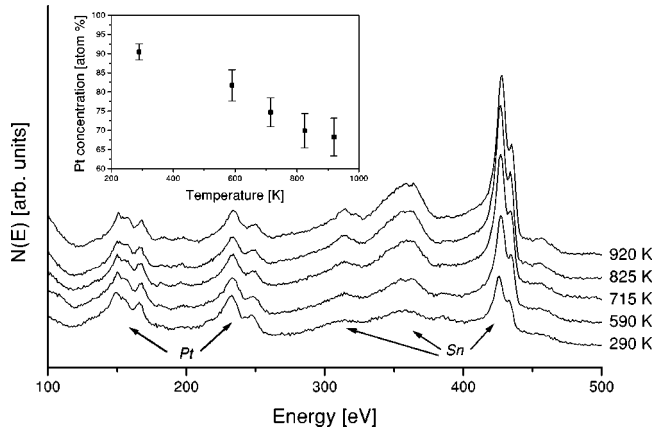


FIG. 1. Integral $[N(E)]$ AE spectra of the sputtered $\text{Pt}_3\text{Sn}(001)$ surface after different annealing treatments. The inset shows the decrease of the Pt surface concentration with annealing evaluated from the AE spectra using the peak-to-peak method of the differentiated $dN(E)/dE$ signal. Electron energy is 10 keV.

move between the main spots upon energy variation. The facets causing these features can be identified with STM. It shows a new type of pyramidal structure not reported previously for this surface (Fig. 3). The sides of the pyramids are (102) facets mainly, as can be seen from the inclination with respect to the (001) plane and the atomic structure. Only near the top of the pyramids is the inclination against the (001) plane lowered, resulting in (104) facets. Atomically resolved images of the facets [Figs. 3(b) and 3(c)] agree in detail with the corresponding “marble” models [Fig. 3(d)].

The bases of the pyramids are oriented parallel to the [100] and [010] surface directions. As can be seen in the overview image [Fig. 3(a)], the size distribution for the pyramids is relatively narrow, with base lengths in a range of approximately 300–400 Å. Some pyramids, however, are significantly larger [a part of such a “giant” pyramid is shown in the lower right corner of Fig. 3(a)]. Base lengths of 1200 Å are common. The height of the smaller, average pyramids is approximately 40–50 Å, whereas large ones can be 200 Å high.

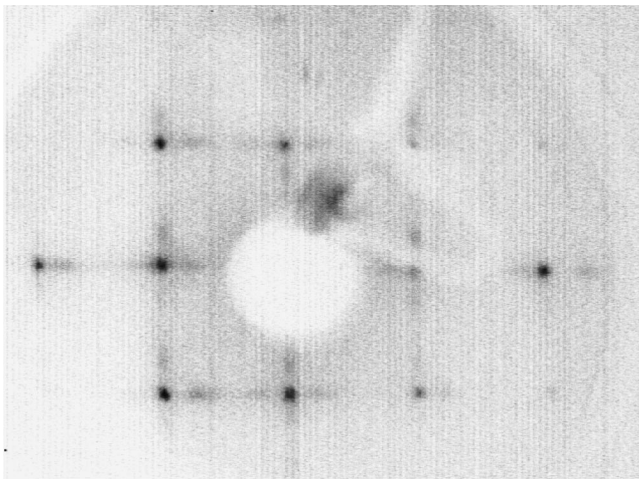


FIG. 2. $c(2 \times 2)$ -LEED pattern at 98 eV of the $\text{Pt}_3\text{Sn}(001)$ surface after low-temperature annealing. The “streaks” surrounding the main spots are indeed facet spots due to the features seen in Fig. 3.

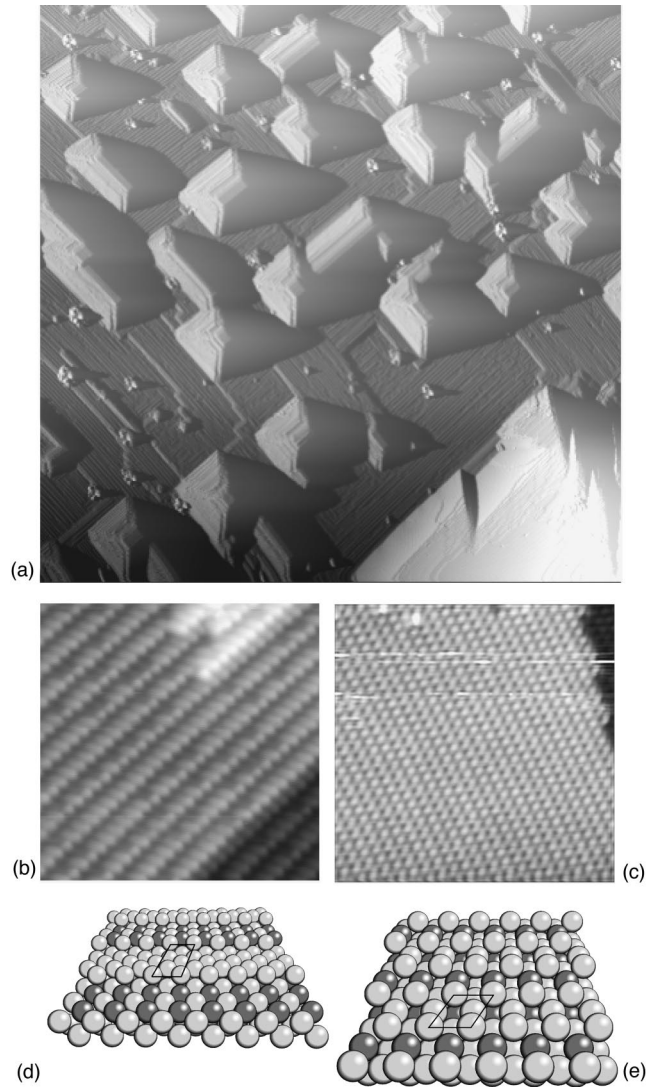


FIG. 3. STM images (a)–(c) and marble models (d),(e) of the $\text{Pt}_3\text{Sn}(001)$ surface after low-temperature annealing. (a) Overview, scan width $(3200 \text{ \AA})^2$, $U_g = 0.9 \text{ V}$, $I_t = 1.0 \text{ nA}$. (b) (104) facet on the side of a pyramid near the top. Scan width $(100 \text{ \AA})^2$, $U_g = 0.2 \text{ V}$, $I_t = 1.0 \text{ nA}$. (c) (102) facet on the side of a pyramid near the base. Scan width $(120 \text{ \AA})^2$, $U_g = 0.4 \text{ V}$, $I_t = 1.0 \text{ nA}$. Marble models of the (104) facet (d) and the (102) facet (e). For better visibility the models correspond to a chemically ordered bulk (Pt atoms light grey, Sn atoms dark grey), whereas the real pyramids are substitutionally disordered in the bulk. The unit cells seen by STM are indicated.

RHEED patterns taken under these conditions show evidence for electrons passing through the pyramids, i.e., transmission RHEED (Fig. 4). The diffraction spots lie on horizontal lines rather than Laue circles (compare schematic drawing in Fig. 4), and they do not move with respect to the shadow edge when changing the angle of incidence. From these patterns, the unit cell of the transmitted crystallites (the pyramids in our case) can be evaluated. We obtain a fcc lattice with a lattice constant of $4.1 \pm 0.3 \text{ \AA}$, consistent with the bulk lattice parameter of 4.00 \AA . Heating to 1000 K results in a normal RHEED pattern with Laue circles and only faint remnants of transmission features. Furthermore, we observe additional half-order spots between the main

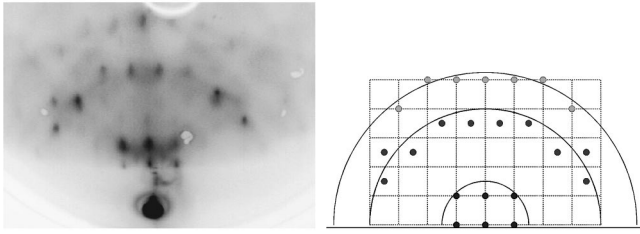


FIG. 4. Experimental (left panel) and schematic (right panel) RHEED pattern of the $\text{Pt}_3\text{Sn}(001)$ surface after low-temperature annealing. The main features are transmission spots lying on horizontal lines rather than Laue circles. The Laue circles are indicated in the schematic pattern. Electron energy is 12 keV, direction of incidence is along [100].

spots of the first Laue zone, indicating long-range chemical order. We then conclude that the pyramids causing the transmission RHEED are substitutionally disordered, compatible with an Sn-depleted surface region.

Looking at the plane parts of the surface between the pyramids, atomic rows are found [Fig. 3(a)]. The same rows are found on top of the pyramids, mainly when they are elongated in one direction, i.e., when the base of the pyramid is a rectangle rather than a square [Fig. 5(b)]. The rows consist of three rows of which the middle one has point defects, giving these structures a “beaded” appearance. The lateral distance of the atoms along the rows is 4.0 Å; the apparent height is 1 Å.

Some pyramids, the more square-shaped ones, show no triple rows on the top. Flat tops exhibiting a square unit cell with a side length of 4 Å are found, as in Fig. 5(a). In the center of a few cells, protrusions can be seen [some are indicated in Fig. 5(a)]. These are very likely Pt atoms at Sn sites. On average, Sn should be present in the center of the square cells but is imaged with very low corrugation and thus appears as a depression (compared to Pt, see discussion). However, since no LEIS or LEED analyses have been performed on the sputtered and low annealed surface, the Sn first-layer concentration for this case is not known. But a high first-layer concentration of Sn is possible even for an overall Sn-depleted surface region, as has been found for the

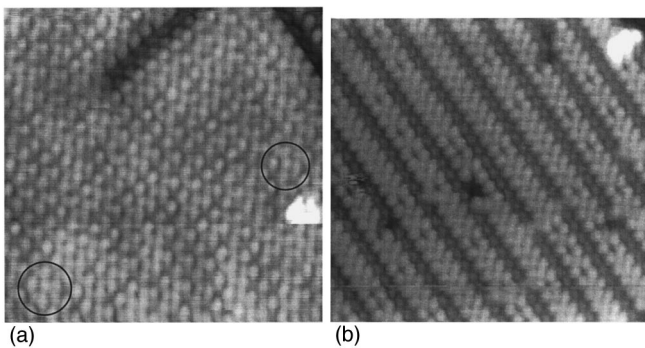


FIG. 5. STM images of a pyramid on $\text{Pt}_3\text{Sn}(001)$. (a) Flat top. Two unit cells with a centered atom are indicated as examples. Usually no centered atom is visible. Scan width $(80 \text{ \AA})^2$, $U_g = 0.5 \text{ V}$, $I_t = 1.0 \text{ nA}$. (b) Examples of “beaded” triple rows on top of pyramids. The distance between the rows is mostly uniform but sometimes larger than shown here. Scan width $(96 \times 100 \text{ \AA})^2$, $U_g = 0.9 \text{ V}$, $I_t = 1.0 \text{ nA}$.

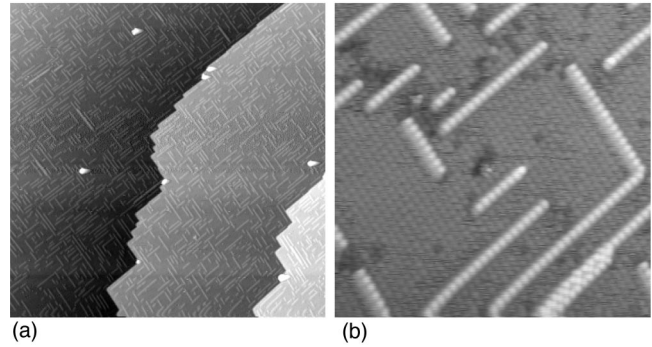


FIG. 6. STM images of the $\text{Pt}_3\text{Sn}(001)$ surface after high-temperature annealing (1000 K). (a) Overview, all steps are double steps running along the [100] and [010] directions. Scan width $(1700 \text{ \AA})^2$, $U_g = 0.9 \text{ V}$, $I_t = 1.0 \text{ nA}$. (b) Close-up view showing the remaining monoatomic rows and the substrate. The apparent height of the rows is 1 Å. The square unit cell of the substrate shows no centered atoms, since only Pt is imaged (see text). Some defects are seen in the upper part of the image. Scan width $(160 \text{ \AA})^2$, $U_g = 10 \text{ mV}$, $I_t = 1.0 \text{ nA}$.

$(\sqrt{3} \times \sqrt{3}) R30^\circ$ reconstruction of $\text{Pt}_3\text{Sn}(111)$.^{11,9,22} Furthermore, vacancies in the center of the square cells seem energetically unfavorable, and the LEED pattern is $c(2 \times 2)$ as for the well-annealed surface (see below), indicating the same unit cell.

Further annealing to 1000 K leads to an improved $c(2 \times 2)$ -LEED pattern with no or reduced streaking. With STM we see a “melting” of the pyramids, whereby the smaller pyramids disappear before the larger ones (in fact, occasional large pyramids always remain). It seems not to be a case of Oswald ripening, i.e., there is no growth of the larger pyramids at the expense of the smaller ones. What remains are large flat terraces decorated with atomic rows along [001] and [010] (Fig. 6). The majority of the rows are monoatomic, only very few double and triple rows are found. These rows are possibly remnants of the beaded rows. The length of the rows is not uniform; maximal lengths are approximately 150 Å. The height of the single rows is 1 Å as for the triple rows. If we look at the flat terraces between the rows, again only a square unit cell with a side length of 4 Å is imaged. Former LEED and LEIS analyses indicate a centered unit cell containing both Pt and Sn,^{7,10} thus, we conclude that only one species is imaged as a protrusion, namely, Pt (see discussion). The corrugation of the centered Sn atom is very low and lost in the residual noise.

All steps found on the well-annealed surface are “double” steps. This is a strong argument for a strict termination with the mixed Pt-Sn layer. In all STM scans we find no evidence for surface-atom mobility within the time resolution of the instrument. All structures including the defects (beading) in the triple atomic rows are stable at room temperature over hours.

IV. DISCUSSION

The (001) surfaces of chemically ordered fcc A_3B alloys have two possible terminations, i.e., in our case, pure Pt or Pt and Sn in a 1:1 ratio. The evidence of all previous work on this surface is that the “mixed” surface prevails.^{5,10,7} STM

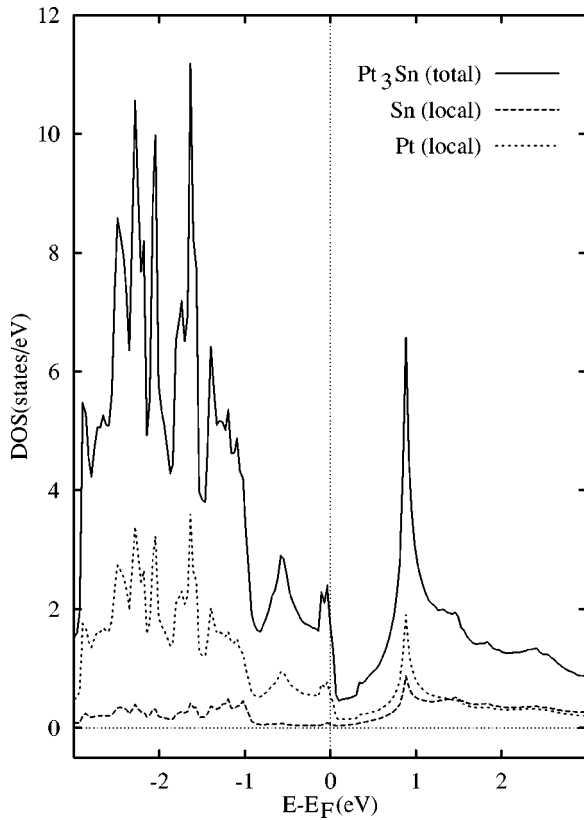


FIG. 7. Total (per unit cell) and local (per space-filling atomic spheres of equal size at both Pt and Sn sites) densities of states of Pt_3Sn , calculated by the tight-binding linear muffin-tin orbitals method (Ref. 39). At positive (sample-) bias voltages the unoccupied states above E_F are imaged in the STM.

topology cannot give *a priori* evidence for the composition. But the formation of double steps on the well-annealed surface is a strong argument for the termination with only one of the possible two truncations. Together with the results of a previous crystallographic LEED analysis¹⁰ and the former LEIS measurements,⁷ the termination with the mixed Pt-Sn plane is obvious. The fact that STM shows only a square unit cell for the well-annealed surface, without evidence for a centered structure, is explained qualitatively by chemical contrast: Due to a considerably lower local density of states (LDOS) at the Sn-atom sites compared to the Pt-atom sites for energies near the Fermi edge (Fig. 7), Pt should be imaged higher than Sn. In fact, this contrast has been observed for the $(\sqrt{3} \times \sqrt{3}) R30^\circ$ structure on $\text{Pt}_3\text{Sn}(111)$,²² where the attribution of the contrast to the chemical elements was unambiguous for stoichiometric reasons. For the $(\sqrt{3} \times \sqrt{3}) R30^\circ$ structure, Sn was even imaged as a depression, indicating indeed a very low LDOS at the Sn sites. In the present work, we have no clear evidence for two species of atoms with different apparent height. Apparently, the remaining noise in the data hinders the imaging of depressions or atoms with lower corrugations in the center of the square unit cells. At considerably higher tunneling voltages ($U_t \geq 1.5$ V), a higher LDOS at the Sn sites should be expected from the bulk band-structure calculations (Fig. 7), but it is generally difficult to achieve atomic resolution on metals at these voltages. Also a bulk band structure can only give a qualitative estimate for the surface LDOS. A calculation

based on the full linear augmented plane-waves method²⁴ (FLAPW) would be required to accurately account for surface effects. So far, this has not been done for Pt_3Sn surfaces.

From topographic considerations, Sn should be imaged higher than Pt, since it is buckled upwards by 0.2 \AA as found by LEIS and LEED,^{7,10} But since STM does not measure the atom core positions, a correlation between apparent and actual height cannot generally be expected. In a recent STM study on $\text{Cu}_3\text{Au}(001)$, however, an upward buckling of Au has been observed¹⁵ in agreement with other reports.^{12,16}

If we assume that the observed contrast is also valid for the structures found on the intermediate annealed surface, we then conclude that the beaded (triple) rows are Pt, too (Fig. 5), as well as the atomic rows on the well-annealed surface of $\text{Pt}_3\text{Sn}(001)$ (Fig. 6). Note that these beaded structures exist between and on top of some pyramids. These features can be considered as “local” reconstruction in order to manage the stress due to the Sn deficit. It should be noted that the single and triple rows run exclusively along the open $[100]$ and $[010]$ directions, not along the close-packed $[110]$ direction. This means that the rows consist of only one atomic species (probably Pt). In the $[110]$ direction, Pt and Sn atoms would alternate.

Assuming that the beaded rows consist of Pt, the hexagonal structure of the rows may be driven by the tendency of Pt to form pseudohexagonal reconstructions as found on Pt(001) (Ref. 25) and Pt-Ni(001) alloys.²⁶ However, the situation is different for Pt_3Sn since no closed layers or larger patches exhibiting a hexagonal structure have been observed. The beaded rows are almost exclusively three atoms wide and separated by a minimum of approximately two lattice constants as seen in Fig. 5.

The well-annealed $\text{Pt}_3\text{Sn}(001)$ surface shows no reconstruction. Only a slight inward relaxation of the first layer and an upward buckling of Sn has been found by LEED.¹⁰ In comparison, for the Pt-Ni(001) surface, a shifted row reconstruction was found²⁶ at certain Pt surface concentrations (Pt-Ni is a substitutionally disordered alloy and different surface concentrations can be prepared by segregation). The driving force for this reconstruction was found to be the tendency of Pt to stay in high coordinated fourfold hollow sites and thereby pushing Ni into nearly on-top bridge sites on the surface. Since Pt_3Sn is a chemically ordered alloy, differences compared to Pt-Ni alloys can be expected. The buckling of Sn already provides the optimal coordination for Pt so that shifted rows (which in a sense can also be regarded as a buckling) are not favorable.

Another finding of the present work is the absence of any long-range superstructure. The $\text{Pt}_3\text{Sn}(111)$ surface, in comparison, shows a hexagonal superstructure due to a dislocation network after the sputtering, i.e., the depletion of Sn in the near surface region.²² This superstructure is actually similar to the one observed for Pt-Ni(111) single-crystal surfaces.²⁷ On $\text{Pt}_3\text{Sn}(001)$, the sputtering leads to the formation of the pyramidal structures (Fig. 3), causing the streaks or facet spots in the LEED pattern (Fig. 2).

In a previous work⁷ the streakiness of the LEED pattern has been attributed to randomly up-and-down step arrays rather than periodically up-and-down arrays. This is, in hindsight, quite a good description of the pyramids with varying

sizes and varying distances in between.

The origin and shape of the pyramids remain to be explained. It is obvious that the pyramidal features are produced by ion bombardment, since at the low annealing temperatures used (600 K; i.e., $\approx 35\%$ of the melting temperature²⁸), the large interlayer mass transport needed to form these three-dimensional structures clearly is not possible. To our knowledge, no study has reported the formation of “positive” (adatom) pyramids after sputtering so far. “Negative” or void pyramids would usually be expected if no layer-by-layer removal takes place. This has been found, e.g., on Cu(001),^{29,30} where also the formation of stable facets for the sides of the voids has been reported.

The question is whether the structures observed on Pt₃Sn(001) can be explained by the same mechanisms that act in pattern formation after sputtering.^{29,31} First, it may be questioned if the pyramidal structures found on Pt₃Sn are, in fact, adatom structures or might also be regarded as void structures. Of course, looking at images like Fig. 3(a), where flat terraces are seen between the pyramids, this interpretation is clearly not appropriate. We note, however, that the surface has been annealed after sputtering (although at low temperature) and, therefore, no longer entirely represents the original sputter morphology. Also, we have observed surface areas where the pyramid density is considerably higher than shown in Fig. 3(a), and no or only a few flat parts were present between the pyramids. If the surface consists exclusively of pyramidal features, it is a matter of convention if one speaks of adatom or void structures. For a sputter process, void formation would generally be expected. So, it may be possible that the adatom pyramids seen in most of our images only appear as adatom structures because the surrounding area has flattened due to annealing. But at this stage this remains speculation, and further experiments are necessary to clearly address the formation process of the pyramids.

Also, it would be interesting to vary the substrate temperature during sputtering and see if the morphologies differ and the inclination of the facets changes. This has been found for ion bombardment of Cu(001),²⁹ where the facets are of (113), (115), or (117) type after sputtering at ≤ 100 K, 200 K, and 325 K, respectively. The features seen in STM images of the same system after room-temperature sputtering³⁰ are also compatible with (117)-like facets. The striking fact is that the same facets are formed during epitaxial growth of Cu on Cu(001),^{32,33} suggesting a common origin of the structures. The formation of stable facets (slope selection) is known from epitaxial growth processes^{32,34,33} and is expected to be a general phenomenon under certain deposition conditions.^{35,36} However, it is not clear *a priori* that structures in growth and ablation are generally complementary as found in the Cu(001) case. The situation should also be more complicated for alloys, where preferential sputtering can often be observed and the atomic species occupy different sublattices (in ordered alloys as Pt₃Sn).

Comparing the (113), (115), and (117) facets found for the (Cu)/Cu(001) system with the (102) and (104) facets found on Pt₃Sn(001), both inclination angle against the substrate and azimuthal orientation are different. Whereas the voids or pyramids on Cu are aligned parallel to the [110] direction, the pyramids on Pt₃Sn are parallel to [100], i.e., rotated by 45°. As a consequence, the local geometry is more

open on (102) and (104) facets in the sense that the step edges are not parallel to close-packed directions (this is valid for all steps found on this surface and also the ones on the completely annealed surface, Fig. 6). Looking at the marble models for the facets in Fig. 3(d), only one species (Pt in the figure) is present at the step edges. Since the pyramids are substitutionally disordered according to RHEED (Fig. 4), the models are not strictly valid. But assuming that Sn is present in the outermost surface and that the chemical short-range order is preserved, they should be applicable at least locally. Thus, the fraction of one preferred species at the step edges could be maximized with step edges running along the open [001] direction. Along the close-packed [110] direction always both Pt and Sn would be present at step edges. Whichever of the two species is preferred at step edges cannot be derived from STM images at the present stage. Because of the chemical contrast between Pt and Sn, we tentatively assume the step edges to be Pt.

One striking fact is the apparent lack of (103)-type facets, which would be inclined by 18.4° against the (001) plane, less than for (102) and more than for (104) facets. These facets could be unstable because of two reasons: (i) Anisotropic diffusion currents could lead to a local increase in inclination as proposed for the growth of Fe/MgO(001).³⁴ This would destabilize certain inclinations, which is generally the origin of slope selection in epitaxial growth, and probably also during sputtering.²⁹ (ii) The lower surface energy for Sn could drive a tendency to prefer facets where Sn atoms are exposed [assuming Pt at the step edges as in Fig. 3(d)]. This would not be the case for (103) facets [and all other (10*N*) facets with *N* odd], therefore they may be avoided. The latter argument implies a sufficiently high surface concentration of Sn, which is compatible with the overall Sn depletion in the surface region as discussed above.

The steeper (101) facet could be unstable for the same reasons. Also, the inclination could be unfavorable for energetic reasons, which would generally favor the low-index surfaces close to (001). Therefore, the shape of the pyramids could also be governed by the tendency to form flat surfaces like (001), on the one hand, and the need for a certain inclination (more open surfaces) for stress relaxation due to the Sn deficit, on the other hand.

V. SUMMARY

The Pt₃Sn(001) surface has been investigated using STM, LEED, AES, and RHEED. After sputtering and annealing at 600 K, the morphology is determined by truncated pyramidal structures with stable facets. At the bottom of the pyramids, (102) facets are found. Near the top, the pyramids flatten and (104)-type facets are formed.

On the flat top of the pyramids, triple atomic rows are found, which exhibit defects in the middle row, giving these structures a “beaded” appearance. These structures could represent a local reconstruction in order to manage the stress due to the Sn deficit of the sputtered surface, which is indicated by the low Sn/Pt AES ratio.

LEED pattern of the not-completely annealed surface shows a $c(2 \times 2)$ structure in agreement with previous reports.^{6,7} The “fine structure” around the fundamental

beams also reported previously could be identified as facet spots due to the pyramids.

RHEED pattern taken under these conditions shows features stemming from transmission through an fcc lattice with a lattice parameter compatible with that of the bulk crystal. No long-range chemical ordering was observed for the pyramids, indicating substitutional disorder, which may be expected for the Sn-depleted surface. However, chemical order must be preserved at least locally according to the $c(2 \times 2)$ pattern in LEED.

Annealing at 1000 K leaves a perfectly ordered flat surface with a well-defined $c(2 \times 2)$ -LEED pattern. Steps are exclusively double steps indicating termination with only one of the possible two truncations, either pure Pt or Pt and Sn in a 1:1 ratio. Previous LEIS and crystallographic LEED studies have clearly favored the mixed termination. This is compatible with STM, if the centered Sn atoms are imaged with very low corrugation and are thus practically lost in the residual noise. This contrast is compatible with bulk band-structure calculations showing a significantly lower LDOS at the Sn sites compared to the Pt sites near the Fermi edge.

On the terraces, atomic row structures running along [100] and [010] are found, consisting of either Pt or Sn. It is

suggestive to assume that the rows are Pt and thus cause the reported catalytic properties. Chemisorption or "titration" experiments could be a way to test for either Pt or Sn.

Further experiments would be required to shed more light on the origin of the pyramidal structures. The morphology is certainly sputter induced, but comparison with existing studies on pattern formation after ion bombardment remains speculative at the present stage. Slope selection due to anisotropic diffusion is a promising concept, and carefully controlling the sputter parameters should give more insight into the underlying processes. Also, the relevance of both the pyramids and the added rows with respect to catalytic activity should be investigated, since cases are known where the more "open" surfaces, e.g., (102), have chemisorption properties that are markedly different from those of low-index surfaces of the same metal.^{37,38}

ACKNOWLEDGMENTS

This work was supported by the DFG and the VIGONI program (DAAD). We would like to thank A. Atrei (Siena, Italy) for fruitful discussions.

- ¹J. Cathro, *J. Electrochem. Soc.* **116**, 1608 (1986).
- ²B. McNicol, R. Short, and A. Chapman, *J. Electroanal. Chem. Interfacial Electrochem.* **72**, 2735 (1976).
- ³F. Dautzenberg, J. Melle, P. Biloen, and W. Sachtler, *J. Catal.* **63**, 119 (1980).
- ⁴Z. Karpinski and J. Clarke, *J. Chem. Soc., Faraday Trans.* **171**, 893 (1975).
- ⁵U. Bardi, L. Pedocchi, G. Rovida, A. Haner, and P.N. Ross, in *Fundamental Aspects of Heterogenous Catalysis Studied by Particle Beams*, edited by H.H. Brongersma and R.A. van Santen (Plenum Press, New York, 1991), p. 393.
- ⁶A.N. Haner, P.N. Ross, and U. Bardi, *Catal. Lett.* **8**, 1 (1991).
- ⁷A.N. Haner, P.N. Ross, and U. Bardi, *Surf. Sci.* **249**, 15 (1991).
- ⁸A.N. Haner, P.N. Ross, and U. Bardi, in *The Structure of Surfaces III*, edited by S.Y. Tong, M.A. Van Hove, K. Takayanagi, and X.D. Xie, Springer Series in Surface Science Vol. 24 (Springer-Verlag, Berlin, 1991), p. 276.
- ⁹W.C.A.N. Ceelen, A.W. Denier van der Gon, M.A. Reijme, H.H. Brongersma, I. Spolveri, A. Atrei, and U. Bardi, *Surf. Sci.* **406**, 264 (1998).
- ¹⁰A. Atrei, U. Bardi, G. Rovida, M. Torrini, E. Zanazzi, and P.N. Ross, *Phys. Rev. B* **46**, 1649 (1992).
- ¹¹A. Atrei, U. Bardi, M. Torrini, E. Zanazzi, G. Rovida, H. Kasamura, and M. Kudo, *J. Phys.: Condens. Matter* **5**, L207 (1993).
- ¹²W.E. Wallace and G.J. Auckland, *Surf. Sci. Lett.* **275**, L685 (1992).
- ¹³T.M. Buck, G.H. Wheatley, and L. Marchut, *Phys. Rev. Lett.* **51**, 43 (1983).
- ¹⁴T.M. Buck, G.H. Wheatley, and D.P. Jackson, *Nucl. Instrum. Methods Phys. Res.* **218**, 257 (1983).
- ¹⁵H. Niehus and C. Achete, *Surf. Sci.* **289**, 19 (1993).
- ¹⁶L. Houssiau and P. Bertrand, *Nucl. Instrum. Methods Phys. Res. B* **115**, 161 (1996).
- ¹⁷D. Sondericker, F. Jona, and P.M. Marcus, *Phys. Rev. B* **33**, 900 (1986).
- ¹⁸D. Sondericker, F. Jona, and P.M. Marcus, *Phys. Rev. B* **34**, 6770 (1986).
- ¹⁹D. Sondericker, F. Jona, and P.M. Marcus, *Phys. Rev. B* **34**, 6775 (1986).
- ²⁰U. Bardi and P.M. Ross, *Surf. Sci. Lett.* **146**, L555 (1984).
- ²¹A. Atrei, L. Pedocchi, U. Bardi, G. Rovida, M. Torrini, E. Zanazzi, M.A. van Hove, and P.N. Ross, *Surf. Sci.* **261**, 64 (1992).
- ²²J. Kuntze, S. Speller, W. Heiland, A. Atrei, I. Spolveri, and U. Bardi, *Phys. Rev. B* **58**, 16 005 (1998).
- ²³*Handbook of Auger Electron Spectroscopy*, edited by C.L. Hedberg (Physical Electronics, Eden Prairie, 1995).
- ²⁴E. Wimmer, H. Krakauer, M. Weinert, and A.J. Freeman, *Phys. Rev. B* **24**, 864 (1981).
- ²⁵A. Borg, A.-M. Hilmen, and E. Bergene, *Surf. Sci.* **306**, 10 (1994).
- ²⁶W. Hebenstreit, G. Ritz, M. Schmid, A. Biedermann, and P. Varga, *Surf. Sci.* **388**, 150 (1997).
- ²⁷M. Schmid, A. Biedermann, C. Slama, H. Stadler, P. Weigand, and P. Varga, *Nucl. Instrum. Methods Phys. Res. B* **82**, 259 (1993).
- ²⁸P. Durussel, R. Massara, and P. Feschotte, *J. Alloys Compd.* **215**, 175 (1994).
- ²⁹H.-J. Ernst, *Surf. Sci.* **383**, L755 (1998).
- ³⁰M. Ritter, M. Stindtmann, M. Farle, and K. Baberschke, *Surf. Sci.* **348**, 243 (1996).
- ³¹S. Rusponi, C. Boragno, and U. Valbusa, *Phys. Rev. Lett.* **78**, 2795 (1997).
- ³²H.-J. Ernst, F. Fabre, and J. Lapujoulade, *Phys. Rev. B* **46**, 1929 (1992).
- ³³L.C. Jorritsma, M. Bijmagne, G. Rosenfeld, and B. Poelsema, *Phys. Rev. Lett.* **78**, 911 (1997).

- ³⁴K. Thürmer, R. Koch, M. Weber, and K.H. Rieder, Phys. Rev. Lett. **75**, 1767 (1995).
- ³⁵M. Siegert and M. Plischke, Phys. Rev. Lett. **73**, 1517 (1994).
- ³⁶K. Thümer, R. Koch, P. Schilbe, and K.H. Rieder, Surf. Sci. **395**, 12 (1998).
- ³⁷G.A. Somorjai and M.A. Van Hove, Prog. Surf. Sci. **30**, 201 (1989).
- ³⁸W.F. Banholzer, Y.O. Park, K.M. Mak, and R.I. Masel, Surf. Sci. **128**, 176 (1983).
- ³⁹O.K. Andersen and O. Jepsen, Phys. Rev. Lett. **53**, 2571 (1984).